Performance Assessment on Board-level Drop Reliability for Chip Scale Packages (Fine-pitch BGA)

Desmond Y.R. Chong[1]*, F.X. Che[2], L.H. Xu[2], H.J. Toh[1,2], John H.L. Pang[2+], B.S. Xiong[2], B.K. Lim[1]

[1]United Test & Assembly Center Ltd (UTAC)
5 Serangoon North Ave 5, Singapore 554916
*Email: yrchong@starhub.net.sg

[2]School of Mechanical & Aerospace Engineering, Nanyang Technological University
50 Nanyang Avenue, Singapore 639798
[+]Email: mhlpang@ntu.edu.sg Tel: 65-67905514

Abstract

Board level drop testing is an effective method to characterize the solder joint reliability performance of miniature handheld products. In this study, drop test of printed circuit boards (PCB) with four-screw support condition was conducted for a 15mmx15mm fine-pitch Ball Grid Array (FBGA) package assembly with solder ball compositions of 36Pb-62Sn-2Ag and Sn-4Ag-0.5Cu on PCB surface finishes of organic solderability preservative, electroless nickel immersion gold and immersion tin. The results revealed a strong influence of different intermetallic compound formation on soldered assemblies drop durability. The lead-based solder supersedes the lead-free composition regardless of the types of surface finish. Joints on organic solderability preservative were found to be strongest for each solder type. Other factors affecting drop reliability such as component location on the board and thermal aging effects are reported.

1. Introduction

With the decrease in size of consumer products such as cellular phones, PDAs, and camcorders, the frequency of accidental drops increases and will cause solder joint cracks in the board assembled Integrated Circuits (IC) packages that eventually leads to malfunction of the product. Research and studies have been conducted for the investigation of the reliability performance of IC packages during drop impact test [1-6]. Work on developing modeling methodologies for failure prediction of solder joints upon drop test are being investigated [7-9]. With the implementation of lead-free solders for the purpose of environmental friendliness, experimentation and analysis focusing on lead-free solder compositions have also been performed and documented [10-13]. Through finite element modeling and analysis, Wong et al [14] identified three main drivers for board level drop impact failure of interconnections; i) elongation and bending of interconnection due to differential flexing of PCB and package, ii) large inertia force from IC packages, and iii) stress waves generated from impact. There is however a lack of documentation in the use of lead-based (Pb-based) and lead-free (Pb-free) solder compositions on different printed circuit board (PCB) pad surface finishes, and their influence on drop impact reliability. The recent drop test study on a 35x35mm PBGA (plastic ball grid array) package by Chong et al [15] showed that different solder alloy of Pb-based and Pb-free when mounted onto different PCB surface finishes resulted in different intermetallics formation and contributed to different failure sites and mode of failure.

Besides solder composition and surface finish, the placement and layout of the IC packages mounted on the PCB also affect drop reliability performance. As reported by Wong et al [14], the package that is mounted near to the support pin of the PCB will subject to exceptionally high acceleration and high magnitude of stress waves transmission through the support pin to the solder joints. Thus the damage may be as significant as the contribution due to differential flexing between the PCB and IC package. Syed et al [8] also showed the joint failure in the IC packages across the PCB is location dependent.

The current work provides an extension to the study by Chong et al [15]. More and more chip scale packages (CSP) are used in miniature handheld products. A new CSP of 15x15mm fine-pitch BGA (FBGA) with 324 solder ball count has been tested. The solder compositions studied are of Pb-based (36Pb-62Sn-2Ag) and Pb-free (Sn-4Ag-0.5Cu), with surface finishes of organic solderability preservative (OSP), electroless nickel immersion gold (ENIG) and Immersion Tin (Im Sn). The study aims to investigate the strength comparison of PCB assemblies of CSP with Pb-based and Pb-free solders onto different surface finishes. The effect of component placement layout across the PCB will also be studied. A comparison on the drop performance of screw and clamp PCB support will be briefly discussed.

2. Test Vehicle and Setup for Drop Impact Test

The Lansmont Model 65/81 drop impact tester (see Fig. 1) was used to carry out the drop test. Solder ball pitch of the 15x15mm FBGA is 0.8mm with ball size of 0.4mm (before reflow). The test package is daisy chained, with full interconnection failure monitoring of the solder balls. Multiple fault isolation pads are designed-in for the purpose of easy identification of failure distribution in the package after the drop test. The packages are mounted on a 77x132mm 2-layer test board with a total thickness of 1.0mm (Fig. 2). Seven packages are mounted in the positions as shown. The solder compositions used in the test are Pb-based of 36Pb-62Sn-2Ag and Pb-free of Sn-4Ag-0.5Cu (also termed as SAC). Five test legs with different PCB surface finishes are classified as follow:

a) Leg 1 - Pb-free on OSP pad finish
b) Leg 2 - Pb-free on ENIG pad finish
c) Leg 3 - Pb-free on Im Sn pad finish
d) Leg 4 - Pb-based on OSP pad finish
e) Leg 5 - Pb-based on ENIG pad finish

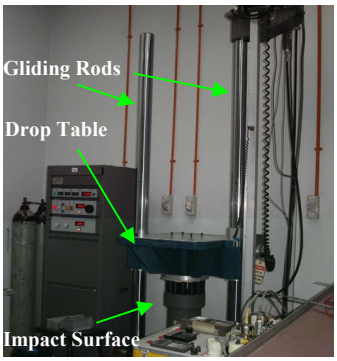

Fig 1. Lansmont Model 65/81 Drop Impact Tester.

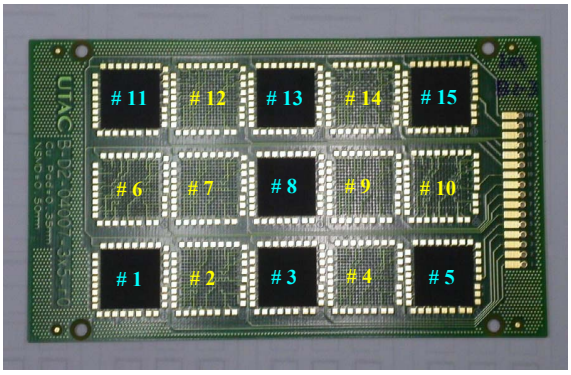

Fig 2. 77x132mm PCB with 15x15mm FBGA Packages.

With board symmetry consideration, the packages are grouped as listed in Table 1 according to their location and distribution across the PCB. This grouping allows the study of the effect of component placement and location on the solder joint's strength, as well as providing more data points per leg for analysis. Three boards were tested for each leg, with the sample size of six, three and twelve for sets "A", "B" and "C" respectively. The drop height was set at 1.0m with the impact surface covered with felt pads. The drop orientation is of horizontal with packages in a face-down position. The test PCB will be screwed onto the drop table at four support pin locations (see Fig. 3). During the test, the drop table is raised and dropped from the desired height along the two guiding rods of the drop tester onto a rigid base covered with layers of felt. Upon impact, the drop responses of interest are the shock level experienced by the drop table and PCB, the bending strain experienced at PCB's center, and the static and dynamic resistances of daisy-chained solder joints in real-time. The peak input shock pulse of the drop table was about 690g in the form of a half-sine shape with 2 millisecond period as shown in Fig. 4. An accelerometer was mounted on the drop table near to the fixture to measure the input acceleration. Another accelerometer was mounted at the center of the PCB (reverse side of the IC package) to characterize the output acceleration response of the PCB. Strain gauges were mounted on the PCB at the opposite side of the center FBGA package. For drop test consistency and repeatability, drop responses of input/output acceleration and PCB strain were monitored for one board from each leg with reproducibility observed.

Table 1. Grouping of Test Units on the PCB.

Group	Package Location	Remarks
"A"	3, 13	"Center Edge"
"B"	8	"PCB Center"
"C"	1, 5, 11, 15	"PCB Corner"

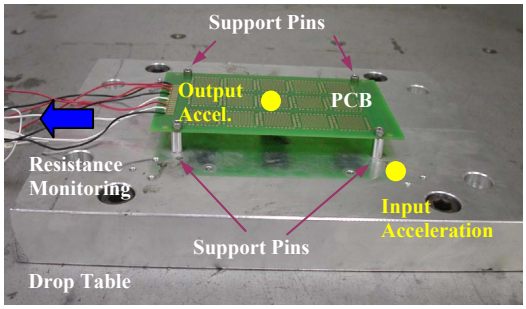

Fig 3. Drop Test Fixture with PCB Mounted onto it.

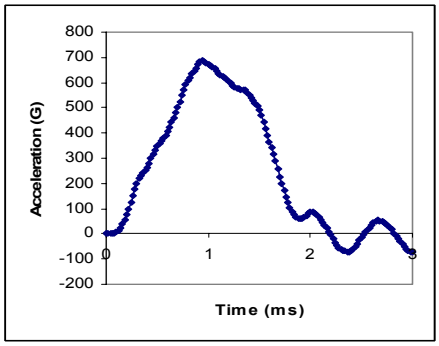

Fig 4. Input Acceleration at the Drop Table Upon Impact.

A dynamic resistance measurement of the daisy-chained solder joints in real-time during drop is used [3,15], where the dynamic resistance, $Rx=Ro/(E/V - 1)$, is represented by a voltage reading on the oscilloscope (four-channels input). When $V \rightarrow E$, $Rx \rightarrow \infty$ (implies an open circuit), it indicates a critical solder joint has failed with crack opening. For this test, R_O=10Ω and E=1.8volts.

3. Results and Discussion

Three sets of test data points are presented with reference to their locations on the PCB, namely "A", "B" and "C". For set "B" where the package is mounted directly at the center of the PCB, it will experience the maximum PCB flexing due to pure bending mode upon impact. As the PCB is supported at 4 corners, the longitudinal edge (length-wise of the PCB) will be subjected to an additional twisting mode instead of the bending mode alone. Thus for the "center-edge" location set "A", the deformation will be constituted by both the bending and twisting modes. For set "C" where it is located near to the support pins, PCB flexing and twisting will be minimal. However, it will experience the highest magnitude of stress wave transmission from the drop table during impact where it can be highly detrimental to the solder joints.

The failure due to opening of solder joints is observed through the change in the dynamic voltage. Before drop, the solder joint resistance (static) was measured by manual probing to ensure no failure in the interconnection is observed. During drop, the solder joint exhibits three phenomena of failure. After cyclic drop test, a solder joint system begins to weaken and a crack will initiate. Further drops will cause the crack to propagate and eventually results in a full crack (termed as *initial* failure). This full crack can cause immediate malfunction of an IC package if the particular joint is of critical functionality. This crack opens when the PCB flexes leading to a resistance discontinuity but closes back to resume electrical continuity after the flexing of the board has ended. This form of observation will be termed as *intermittent* solder joint failure, where static resistance measurement is not able to register any discontinuity. When the crack becomes larger and cannot be closed back even after the impact test, a *permanent* solder joint failure will be resulted (open circuit registered with static resistance measurement). The *initial* failure is identified as the failure criteria for current test.

3.1. Dynamic Responses and Observations

In any drop, the solder joints resistance (or "voltage") for the FBGA packages and PCB bending strain were captured. A typical curve response is showed in Fig. 5 where it can be divided into two regions, before impact (static) and after impact (dynamic). Test result for Leg 5 (Pb-based/ENIG) at the 78th drop is used for illustration. Channel 1 is used for dynamic strain measurement at the PCB center. Channels 2, 3 and 4 are measuring the dynamic voltages of package units 1, 8 and 15 respectively. One large division in the y-axis of the oscilloscope corresponds to 1.0 volt (V). Before impact, the PCB strain is zero while the static solder joint resistance is similar to the value measured by manual probing. Each package location has its own zero-reference voltage and initial voltage reading of 0.6V [$Rx(initial) = 10/(1.8/0.6 - 1) = 5\Omega$] as indicated. With reference to channel 3 (unit 8), a peak voltage was registered after impact, indicating that an *initial* failure in a solder joint has occurred. The following fluctuation in peaks was constituted by the downward/upward flexing of the PCB leading to the opening/closing mode of the crack. When flexing of the board has ended, static resistance measurement by manual probing was not able to register any discontinuity. This observation describes the *intermittent* solder joint failure. With it, unit 8 of Leg 5 registered a failure at the 78th drop. At subsequent drops, unit 8 would register fluctuation in voltage reading. At the 89th drop, it registered a maximum voltage of 1.8V [$Rx(final) = \infty$]. The discontinuity was confirmed by manually probing with an open circuit being measured, thus implying that the joint opening is *permanent*. Similar observation was made for unit 15 of channel 4. Joint failure also occurred at 78th drop. For channel 2 (unit 1), the solder joints remained intact as there was no change in the resistance responses before and after the impact. The drop cycles constituted to the *initial* failure of the solder joint was recorded for results compilation and analysis.

High speed digital camera was employed to capture the drop impact images of the test boards upon impact. Fig. 6 shows the PCB bending sequence. The drop table will be put to a sudden stop upon impact with the rigid base, whereas the PCB continues to travel downwards leading to the concave bending mode of the board. Due to its inertia and flexibility, the PCB will reflex back to a convex bending mode. This concave/convex bending mode will continue and eventually subside after sometimes due to damping effects experienced by the PCB. The amplitudes of the initial concave and convex bending are the highest, corresponding to Figs. 6b and 6c respectively.

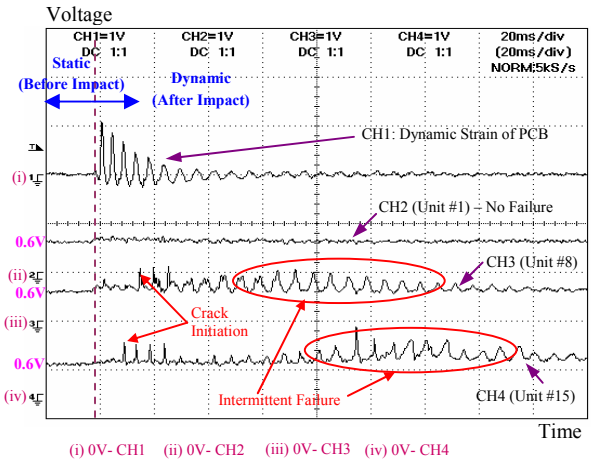

Fig 5. Typical Dynamic Responses for Drop Test - Leg 5 (Pb-based on ENIG) at 78th Drop.

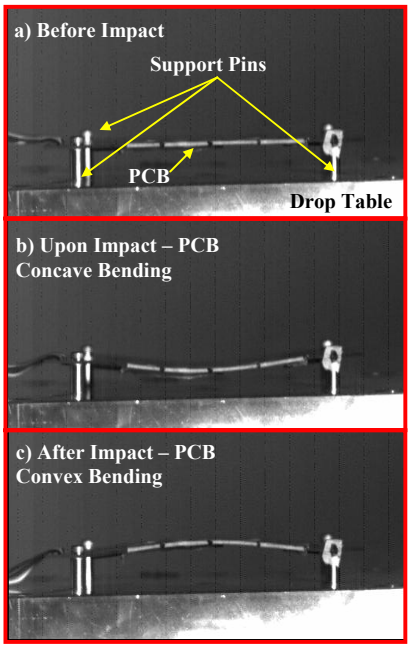

Fig 6. High Speed Digital Images of PCB Bending for Horizontal Orientation Drop.

3.2. Drop Test Results and Trends

The drop test was conducted until all the units on the board had failed. The average number of drop cycles to *initial* failure for each three groups in different legs is reported, with the failure trend and performance plotted in Fig. 7. In the first instance, drop reliability of the Pb-based solder composition

supersedes the Pb-free composition regardless of the types of surface finish. The solder joint formation (both Pb-based and Pb-free) on OSP finish was found to be strongest as compared to ENIG and Im Sn. For the Pb-free legs, Im Sn surface finish generated the lowest drop cycles to failure. The above failure trend can be attributed to the type of intermetallic compound (IMC) layer formed at the solder joint interface with the PCB copper pad, and will be discussed in the next section.

The test results also captured the location dependent failure trend of the solder joints. Packages in group "A" located at the PCB center edge suffered the most drop impact damage. Due to the large deformation constituted by both the bending and twisting modes, the solder joints experienced the highest level of stress where all the solder joints failed below the drop cycles of twenty. Study by Syed et al [8] revealed similar observation. In their test the PCB is fully populated with fifteen components, and solder joints at location #14 (refer to Fig. 2) failed earlier than of #8. In the current test with no component mounted at locations of #2, 4, 12 and 14, units #3 and 13 took the additional stress induced by the twisting mode of the PCB. Packages at the PCB center and corner were found to exhibit equal chance of joint failure. Crack failure in packages at the PCB center was caused by the pure bending of the board, with the tensile stress experienced tearing the joints apart. For packages at the PCB corner, PCB flexing and twisting will be minimal. The solder joints were damaged by the impact stress waves transmitted from the drop table through the support pins. In addition, the PCB adjacent to the support pins could experience up to a thousand times acceleration (1000g) and similarly for a package near to it. Whereas a package located at center on the same PCB, its acceleration could only be in the range of hundreds of gravitational acceleration. Thus given the same mass, interconnects in the package placed near the support will be subjected to a larger tensile stress and eventually lead to impact failure.

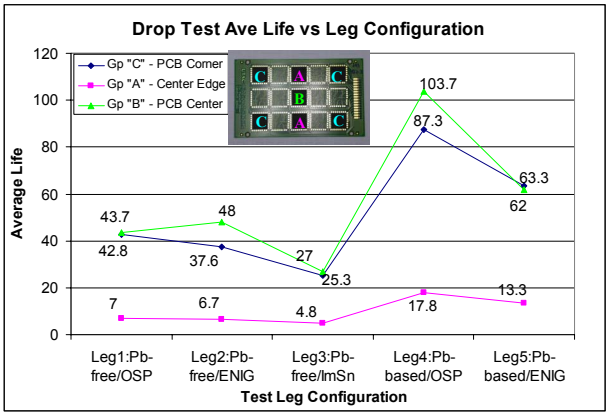

Fig 7. Drop Test Failure Cycles for Different Test Legs.

Fig. 8 shows the solder joints failure distribution across the PCB. Due to pure bending mode in location "B", joints at corner of the package failed as a result. Damage by stress wave transmission through the support pins was evidently demonstrated for units in group "C", where joints at the package corner had failed. For group "A", failure was registered at left and right rows of the package. The failure location mapping was preformed after all units in a single board had failed. Thus it may have failed to capture the first solder joint crack occurring at the corner of the package (shaded in green). The subsequent drop cycles resulted in adjacent joints to fail. Similar failure distribution was observed in all test legs.

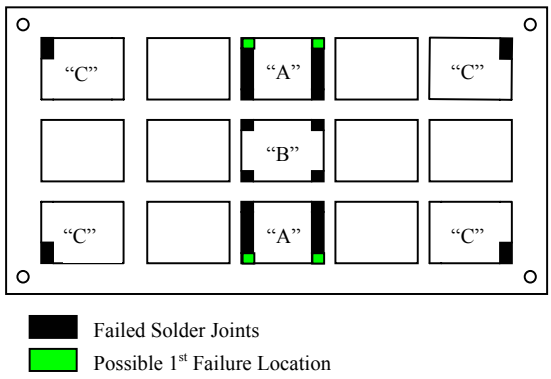

Fig 8. Solder Joints Failure Distribution Across the PCB.

3.3. Failure Analysis of Solder Joints

Solder joints corresponded to failed locations in Fig. 8 were sent for cross-sectioning to determine the failure sites. The test results revealed the solder joint's strength in the rank of: Pb-based/OSP > Pb-based/ENIG > Pb-free/OSP > Pb-free/ENIG > Pb-free/Im Sn. Chong et al [15] reported the influence of IMC formation on solder joint drop durability. The different IMC layer formations are illustrated in Fig. 9. When Pb-based or SAC solder reflowed over an OSP copper pad, the OSP coating is evaporated and allows the interaction of the solder with copper to form a binary intermetallic of Cu_6Sn_5 [16-18]. For SAC soldered onto Im Sn surface finish, intermetallic of CuSn would be formed as well. During soldering process onto the ENIG finish, the gold plating (usually < 1um) will dissolve rapidly into the solder. And the nickel barrier layer forms a binary and ternary intermetallic of Ni_3Sn_4 [19] and Cu-Ni-Sn [20-21] for the Pb-based and SAC solder compositions respectively.

Brittle fracture is promoted through the suppression of plastic deformation under high strain rate test situations [22]. Thus with drop test for soldered assemblies which is of high strain rate in nature, it usually causes brittle failure in the IMC layer instead of ductile failure in the solder. Fig. 10 describes the different failure sites of the FBGA package solder joints. Solder joint crack at the interface of solder to PCB copper pad were found in all the legs, with the exception of Leg 4 (Pb-based on OSP). It is postulated that the Cu_6Sn_5 IMC formed due to Pb-based solder on OSP finish is much thinner as compared to SAC solder reflowed on OSP and Im Sn surfaces. A higher reflow temperature is required for the SAC solder (typically 260°C peak vs 225°C for Pb-based solder), thus it may promote thicker IMC growth in Leg 1. For SAC solder reflow on Im Sn surface (Leg 3), the Sn existed on the copper pad would further aggregate the formation of thick Cu_6Sn_5 layer. The extra thick and brittle Cu_6Sn_5 layer could

result in quick damage under impact loading thus generating a worse off drop performance. Instead of joint interface failure at the PCB side for Leg 4, the crack has migrated to PCB resin and joint interface at the package side. Similar explanation could be offered for solder reflow on ENIG surface finish. IMC of Ni_3Sn_4 and Cu-Ni-Sn are both very brittle in nature. Thus a thicker layer of Cu-Ni-Sn formed in Leg 2 will be more prone to impact failure as compared to Leg 5. PCB resin crack was also observed in Leg 5.

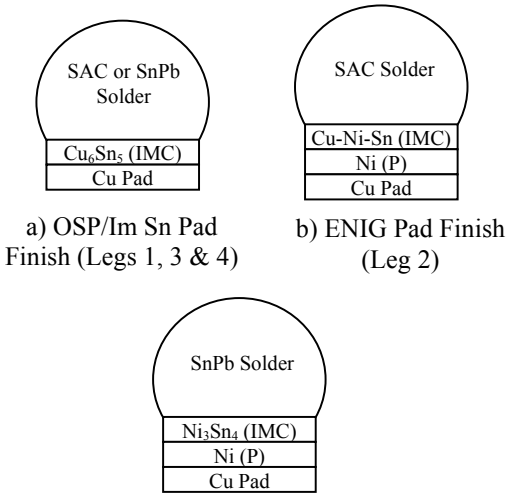

a) OSP/Im Sn Pad Finish (Legs 1, 3 & 4)

b) ENIG Pad Finish (Leg 2)

c) ENIG Pad Finish (Leg 5)

Fig 9. Intermetallic Compound Layers Formation for Legs 1-5.

3.4. Thermal Aging Effect on Solder Joints Reliability

Thermal aging factors affecting drop reliability of i) isothermal aging at 150°C with different periods of 120, 240 and 390 hours, and ii) thermal cycling from –40°C to 125°C with different cycles of 500, 1000 and 1500, are reported for the SAC/OSP and SAC/ENIG legs. For this analysis, the maximum drop cycle to *permanent* failure was used. The drop lifetime decreased significantly after thermal aging. The reliability could degrade by more than 50% after 500 thermal cycles or 120 hours isothermal aging. This is even more significant after longer thermal aging time. For SAC/OSP after 1000 and 1500 thermal cycles, or after isothermal aging of 240 and 390 hours, the drop impact lifetime went down to about 5 drops or even lower. The proposed reason for the decrease in drop impact life is the thicker IMC growth after undergoing thermal aging processes.

The drop reliability of SAC/ENIG leg appears to perform better than SAC/OSP after thermal cycling aging. For as reflowed specimens of units 3 and 13 shown in Fig. 11, the lifetime for SAC/OSP (29 drops) was better than SAC/ENIG (21 drops). The drop impact lifetime decreased significantly from 29 to 6 for SAC/OSP after 500 thermal cycles. And after 1000 and 1500 thermal cycles, the specimen can only withstand one drop before failure occurs. The drop lifetimes for SAC/ENIG after 500, 1000 and 1500 thermal cycles were 13, 9 and 8 respectively, which were obviously better than SAC/OSP. The reason is attributed to the slower growth rate of Cu-Ni-Sn IMC (thus a thinner layer) as compared to Cu_6Sn_5 IMC with rapid growing rate, where brittle failure in the IMC layer is the main contribution to drop impact solder joint failure.

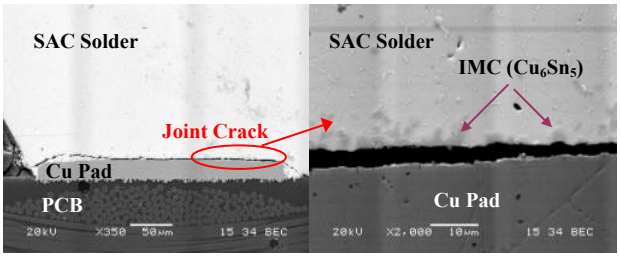

a) Leg 1 – Pb-free on OSP

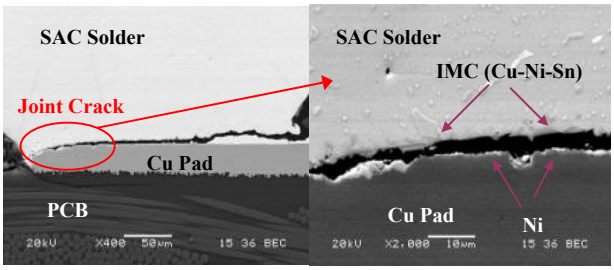

b) Leg 2 – Pb-free on ENIG

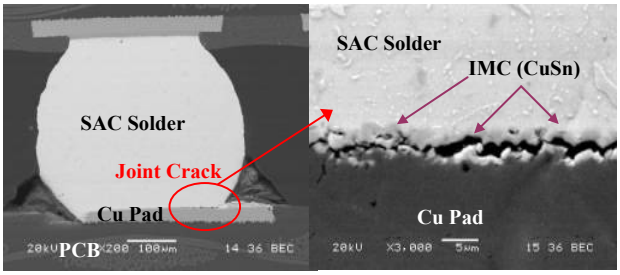

c) Leg 3 – Pb-free on Im Sn

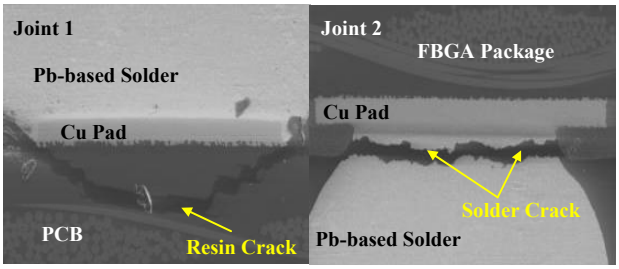

d) Leg 4 – Pb-based on OSP

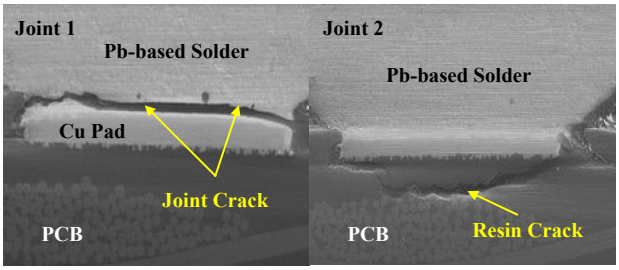

e) Leg 5 – Pb-based on ENIG

Fig 10. Cracks and Failures Found in the Solder Joint System.

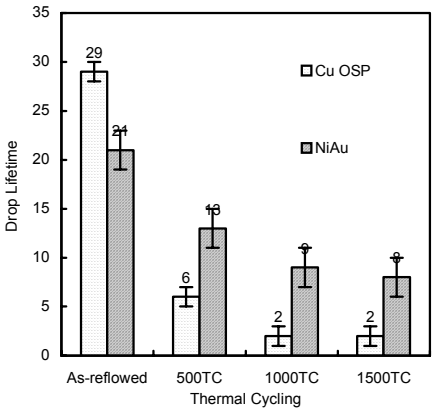

Fig 11. Drop Lifetime for Units #3 and #13 Before and After Thermal Cycling Aging.

4. FE Modeling for FBGA Pb-free Solder Joints

Finite element (FE) simulation of the FBGA assembly with Pb-free solder was performed to investigate the stress-strain behavior of the solder joints during drop test. Assumption was made that the first vibration mode is dominant for the FBGA specimen subjected to drop impact load. Therefore a 3-dimensional quarter model was used in this study with symmetric boundary conditions prescribed as shown in Fig. 12a. Clamped support condition was also modeled for comparison. The materials considered in FE simulation include FR4 PCB, SAC solder, copper pads on both the board and package sides, BT substrate, silicon die and mold compound. For solder joint located at package corner where it is more critical than others, finer mesh was used with the remaining solder array of coarser meshing (illustrated in Fig. 12b). The input acceleration from experimental measurement per Fig. 4 was applied onto the PCB support location. A total of 15 microseconds was simulated. Strain rate dependent material properties of the SAC solder were implemented in FE modeling [23].

It was found from FE simulation results that the stress or strain on PCB side was higher than on package side due to PCB deflection effect, thus indicating the solder/PCB interface is more prone to fail. As such, emphasis is placed on solder at the solder/PCB interface for subsequent analyses. Fig. 13 shows the component stress in drop direction and first principal stress of the critical node on PCB side for the 4-screw support condition. It can be seen that peaks for component peel stress (SY) and first principal stress (S1) are quite close, which implies that the peel stress is the dominant part in inducing crack initiation or failure at solder/PCB interface. It was observed from experiment that PCB board exhibits more bending for 4-screw support condition than the clamped support case. The FE modeling result in Fig. 14 also shows that the output acceleration of the PCB board center is higher for the 4-screw support than that of clamped support case when subjected to the same input acceleration. Thus for the FBGA assembly under 4-screw support when compared to the clamped support case, it is more prone to drop failure due to the larger deflection of PCB center and higher inertial force of FBGA located at PCB center. From the solder stress point of view, the 4-screw support condition also resulted in higher stress level than the clamped support case (as shown in Fig. 15). Fig. 16 shows the effective plastic strain of the critical solder node on board side. The larger plastic deformation of solder occurring in the 4-screw support condition will induce much early drop failure at the solder/PCB interface than the clamped support case.

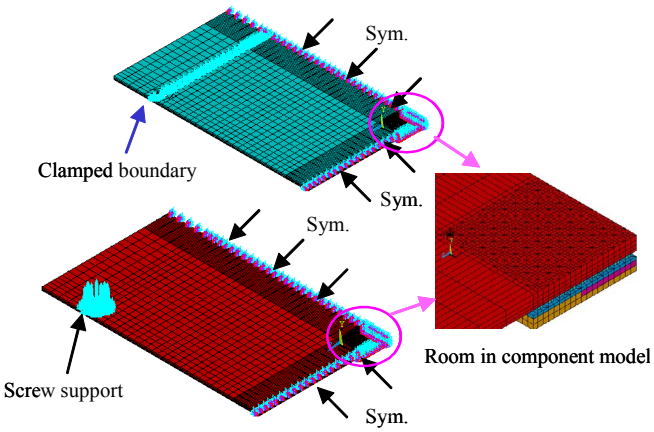

Fig 12a. 3D Quarter FE Model and Boundary Conditions for the FBGA Specimen.

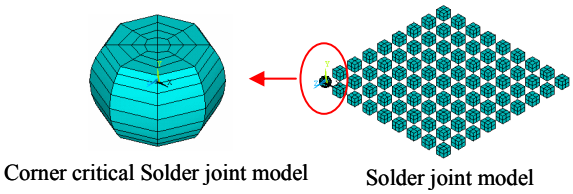

Fig 12b. Fine and Coarse Meshing for Corner and Rest of the Solder Joint Array.

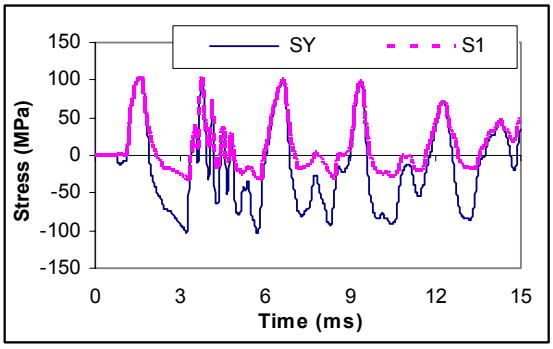

Fig 13. Peel (SY) and First Principal (S1) Stresses of Critical Node for 4-screw Support Condition.

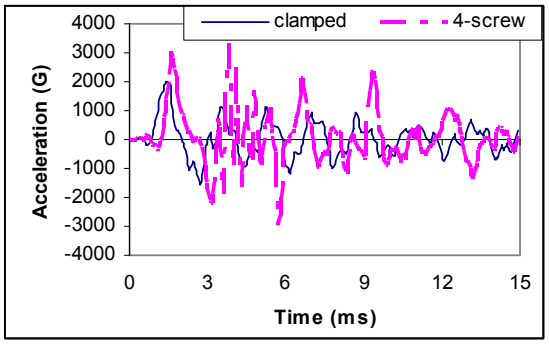

Fig 14. Output Acceleration of the PCB Center for Different Support Conditions.

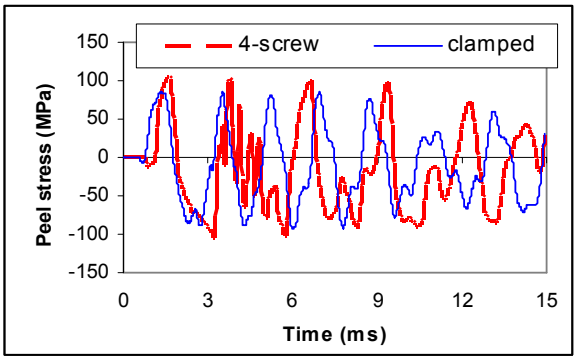

Fig 15. Peel Stress of Critical Node for Different Support Conditions.

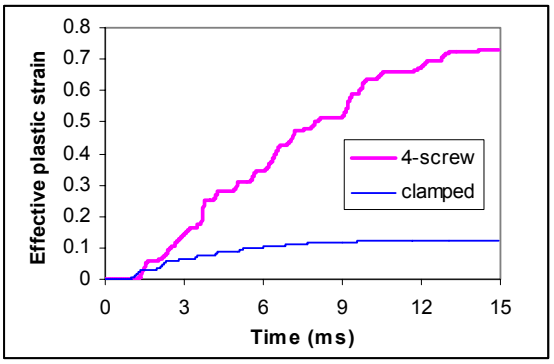

Fig 16. Effective Plastic Strain of Critical Solder Node for Different Support Conditions.

5. Conclusions

The drop impact reliability performance of the 15x15mm CSP (FBGA type with 324 solder balls) has been assessed for solder compositions of 36Pb-62Sn-2Ag and Sn-4Ag-0.5Cu onto surface finishes of OSP, ENIG and Im Sn. The drop responses mechanism, failure distribution and sites have been analyzed. The following conclusions can be drawn:

i) Combination of bending and twisting modes in the 4-screw support PCB during drop impact will constitute to the highest level of stress leading to early joint crack failure.

ii) Failure rate and distribution of the IC packages mounted onto a PCB is location dependent.

iii) A strong influence of different IMC formation on soldered assemblies drop durability.

iv) The solder joint formation (both Pb-based and Pb-free) on OSP finish was found to be strongest as compared to ENIG and Im Sn.

v) Based on current test vehicles, drop reliability of the Pb-based solder composition supersedes the Pb-free composition regardless of the type of surface finishes.

vi) Thermal aging will degrade drop reliability of the solder joints significantly.

vii) FE simulation results show that a solder joint is more prone to failure on the PCB side. The larger plastic deformation of solder and higher joint stress experienced by the 4-screw support condition will induce much early drop failure at the solder/PCB interface than the clamped support case.

Acknowledgments

This work was conducted under a research collaboration project between UTAC and NTU. The authors would like to thank Dr. Anthony Sun and CK Wang for the support of the research project, and acknowledge the support of the School of Mechanical and Aerospace Engineering at Nanyang Technological University through the Electronics Packaging Strategic Research Program.

References

1. D.J. Xie, M. Arra, S. Yi, D. Rooney, "Solder Joint Behavior of Area Array Packages in Board Level Drop for Handheld Devices", *Proc 53rd Electronic Components and Technology Conf*, New Orleans, LA, May 2003, pp. 130-135.
2. Y.Q. Wang, K.H. Low, F.X. Che, H.L.J. Pang, S.P. Yeo, "Modeling and Simulation of Printed Circuit Board Drop Test", *Proc 5th Electronics Packaging Technology Conf,* 2003, pp. 263-268.
3. J. Luan, T.Y. Tee, E. Pek, C.T. Lim, Z.W. Zhong, "Modal Analysis and Dynamic Responses of Board Level Drop Test", *Proc 5th Electronics Packaging Technology Conf,* 2003, pp. 233-243.
4. L. Zhu, W. Marcinkiewicz, "Drop Impact Reliability Analysis of CSP Packages at Board and Product System Levels Through Modeling Approaches", *Proc Inter Society Conference on Thermal Phenomena*, 2004, pp. 296-303.
5. P. Lall, D. Panchagade, Y. Liu, W. Johnson, J. Suhling, "Models for Reliability Prediction of Fine-Pitch BGAs and CSPs in Shock and Drop-Impact", *Proc 54th Electronic Components and Technology Conf*, Las Vegas, NV, June 2004, pp. 1296-1303.
6. Q. Yu, K. Watanabe, T. Tsurusawa, M. Shiratori, "The Examination of the Drop Impact Test Method", *Proc Inter Society Conference on Thermal Phenomena*, 2004, pp. 336-342.
7. T.Y. Tee, H.S. Ng, C.T. Lim, E. Pek, Z.W. Zhong, "Impact Life Prediction Modeling of TFBGA Packages under Board Level Drop Test", *Journal of Microelectronics Reliability*, Vol. 44, Issue 7, July 2004, pp. 1131-1142.

8. A. Syed, S.M. Kim, W. Lin, J.Y. Khim, E.S. Song, J.H. Shin, T. Panczak, "A Methodology for Drop Performance Prediction and Application for Design Optimization of Chip Scale Packages", *Proc 55th Electronic Components and Technology Conf*, Lake Buena Vista, FL, June 2005, pp. 472-479.
9. P. Lall, D. Panchagade, P. Choudhary, J. Suhling, S. Gupte, "Failure-Envelope Approach to Modeling Shock and Vibration Survivability of Electronic and MEMS Packaging", *Proc 55th Electronic Components and Technology Conf*, Lake Buena Vista, FL, June 2005, pp. 480-490.
10. M. Arra, D.J. Xie, D. Shangguan, "Performance of Lead-Free Solder Joints Under Dynamic Mechanical Loading", *Proc 52nd Electronic Components and Technology Conf*, 2002.
11. M. Amagai, Y. Toyoda, T. Ohnishi, S. Akita, "High Drop Test Reliability: Lead-free Solders", *Proc 54th Electronic Components and Technology Conf*, Las Vegas, NV, June 2004, pp. 1304-1309.
12. T. Chiu, K. Zeng, R. Stierman, D. Edwards, K. Ano, "Effect of Thermal Aging on Board Level Drop Reliability for Pb-free BGA Packages", *Proc 54th Electronic Components and Technology Conf*, Las Vegas, NV, June 2004, pp. 1256-1262.
13. S.K. Saha, S. Mathew, S. Canumalla, "Effect of Intermetallics Phases on Performance in a Mechanical Drop Environment: 96.5Sn3.5Ag Solder on Cu and Ni/Au Pad Finishes", *Proc 54th Electronic Components and Technology Conf*, Las Vegas, NV, June 2004, pp. 1288-1295.
14. E.H. Wong, K.M. Lim, N. Lee, S. Seah, C. Hoe, J. Wang, "Drop Impact Test – Mechanics & Physics of Failure", *Proc 4th Electronics Packaging Technology Conf*, 2002, pp. 327-333.
15. D.Y.R. Chong, K. Ng, J.Y.N. Tan, P.T.H. Low, J.H.L. Pang, F.X. Che, B.S. Xiong, Luhua Xu, "Drop Impact Reliability Testing for Lead-Free and Leaded Soldered IC Packages", *Proc 55th Electronic Components and Technology Conf*, Lake Buena Vista, FL, June 2005, pp. 622-629.
16. A.C.K. So, Y.C. Chan, "Reliability Studies of Surface Mount Solder Joints – Effect of Cu-Sn Intermetallic Compounds", *IEEE Transactions on CPMT*, Part B, Vol. 19, No. 3, August 1996, pp. 661-668.
17. M. Lee, Y. Hwang, M. Pecht, J. Park, Y. Kim, W. Liu, "Study of Intermetallic Growth on PWBs Soldered with $Sn_{3.0}Ag_{0.5}Cu$", *Proc 54th Electronic Components and Technology Conf*, Las Vegas, NV, June 2004, pp. 1338-1346.
18. G.Y. Li, B.L. Chen, "Formation and Growth Kinetics of Interfacial Intermetallics in Pb-Free Solder Joint", *IEEE Transactions on CPT*, Vol. 26, No. 3, September 2003, pp. 651-658.
19. Y.C. Chan, P.L. Tu, C.W. Tang, K.C Hung, J.K.L. Lai, "Reliability Studies of uBGA Solder Joints – Effect of Ni-Sn Intermetallic Compound", *IEEE Transactions on AP*, Vol. 24, No. 1, February 2001, pp. 25-32.
20. S. Dunford, S. Canumalla, P. Viswanadham, "Intermetallic Morphology and Damage Evolution under Thermomechanical Fatigue of Lead (Pb)-Free Solder Interconnections", *Proc 54th Electronic Components and Technology Conf*, Las Vegas, NV, June 2004, pp. 726-736.
21. Y. Zheng, C. Hillman, P. McCluskey, "Intermetallic Growth on PWBs Soldered with Sn3.8Ag0.7Cu", *Proc 52nd Electronic Components and Technology Conf*, 2002.
22. M.A. Meyers, "Dynamic Behavior of Materials", John Willey, 1994.
23. J.H.L. Pang, F.X. Che, "Drop Impact Analysis of Sn-Ag-Cu Solder Joints Using Dynamic High-Strain Rate Plastic Strain as the Impact Damage Driving Force", *Proc 56th Electronic Components and Technology Conf*, San Diego, CA, June 2006.